International Journal of Smart Energy Technology and Environmental Engineering
Volume 3, Issue 1, March 2024
https://setee.globalpublisher.org/
http://globalpublisher.org/journals-1007/

Analytical solution of the steady magnetohydrodynamic (MHD) free convection flow over a semi-infinite flat vertical plate moving in a porous medium with viscous dissipation

Behshad Shishehbor[1,*] - Behnam Shishehbor[2]
1- Mechanical Engineering Department, Islamic Azad University, South Tehran Branch, Tehran, Iran
2- Civil Engineering Department, Islamic Azad University, South Tehran Branch, Tehran, Iran
*Corresponding Author: st_b_shishehbor@azad.ac.ir

ABSTRACT

The present study aims to discuss the analytical solution of the steady MHD free convection flow over a semi-infinite flat vertical plate moving in the presence of a magnetic field embedded in a porous medium with viscous dissipation under the Soret and Dufour effects. Soret and Dufour effects depend on the fluid density and its changes and therefore, these effects appear when the fluid density on the surface of the plate is less than the fluid density around the plate (medium). In this study, the governing equations in the form of differential equations higher than one have been solved by direct method with the guessing of the private answers using the perturbation technique and the boundary conditions applied in the problem. Finally, the concentration, temperature and velocity profiles have changed as a result of changes in the parameters such as magnetic parameters, magnetic permeability, Grashof, Prandtl, Eckert, Schmidt, Dufour and Soret numbers which, in turn, have caused some changes in the Sherwood, Nusselt numbers and skin-friction coefficient, and they have been shown by graphs and tables.

Keywords: Analytical solution, MHD, Free convection, Vertical plate, Viscous dissipation,

1. INTRODUCTION

In recent years, the use of MHD has increased in various fields including engineering sciences such as electronics, mechanics, metallurgy, chemistry and etc. and space sciences such as astronomy, geophysics, astronomy, etc. In the engineering sciences, this method has been frequently used in the accelerators to speed up, and in the fields of heat transfer, preventing heat dissipation, increasing turbine efficiency, reducing head drop in the pipelines and in the magnetic generators in order to convert thermal and kinetic energy to electricity. Many applications are presented in the field of heat and heat exchangers. For example, in the case of heat transfer, MHD effects on the conductive fluids flow increase the velocity, temperature and

concentration, and it sometimes happens conversely. In fact, it can be said that MHD affects the heat transfer parameters, which these effects change the behavior of the conductive fluid flow regime. Most recently, researchers have done several researches on heat transfer affected by MHD. Wahiduzzaman et al. (2015) have examined the numerical solution of MHD convection and mass transfer flow of an incompressible viscose fluid about an inclined plate with Hall current and constant heat flux [1]. Wahiduzzaman et al. (2015) have investigated the MHD flow over an inclined rotating plate with a variable reactive index [2]. Khan et al. (2012) have examined the non-Newtonian MHD mixed convective power-law fluid flow over a vertical stretching sheet with thermal radiation, heat generation and chemical reaction effects [3]. Saha et al. (2011) have studied the effects of Hall current on MHD natural convection flow from a permeable flat vertical plate with a uniform surface heat flux [4]. Samad and his colleague (2009) have investigated the MHD heat and mass transfer of free convection flow along a vertical stretching sheet in presence of magnetic field with heat generation [5]. Das et al (2009) have examined the mass transfer effects on MHD flow and heat transfer past a vertical porous plate through a porous medium under oscillatory suction and heat source [6]. Aboeldahab and his colleague (2001) have done a study about Hall current effect on magneto hydrodynamic free convection flow past a Semi-Infinite plate with mass transfer [7]. Soret effect arises due to the difference in density, so this effect is used to isolate the isotope in the mixture of gases. About this effect, it can be said that mass flux can be created by thermal gradients, which means the Soret thermal effect. Dufour effect depends on thermal emission and is equal to the ratio of the concentration gradient to the thermal flux in the flow. Both Soret and Dufour effects are very effective, and sometimes they cannot be ignored with a low numerical value, and their effect on the flow increases the concentration and temperature. Gangadhar (2013) has investigated Soret and Dufour effects on MHD and heat transfer over a vertical plate with a convective surface boundary condition and chemical reaction [8.. Karim et al. (2012) have examined Soret and Dufour effects on steady MHD flow in presence of heat generation and magnetic field past an inclined stretching sheet [9]. Tai and his colleague (2010) have examined Soret and Dufour effects on free convection flow of non- Newtonian fluids along a vertical plate embedded in a porous medium with thermal radiation [10]. Reddy and his colleague (2010) have studied Soret and Dufour effects on steady MHD free convection flow past a semi-infinite vertical plat in a porous medium with viscous dissipation which this research has been numerically solved using Runge-Kutta (order 4) method through the Shooting technique [11]. Tsai and his colleague (2009) have performed numerical study of Soret and Dufour effects on heat and mass transfer from natural convection flow over a vertical porous medium with variable wall heat fluxes [12]. Postelnicu (2004) has investigated influence of a magnetic field on heat and mass transfer by natural convection from vertical surface in porous media considering Soret and Dufour effects [13].

In recent years, many researches and articles have been presented in the area of analytical solution of the issues about MHD. Omowaye et al. (2015) have examined Dufour and Soret effects on steady MHD convective flow of a fluid in a porous medium with temperature dependent viscosity through Homotopy Analysis Method [14]. Raju et al. (2014) have performed analytical study of MHD natural convective flow of dissipative boundary layer past a porous vertical surface in the presence of thermal radiation, chemical reaction and constant suction [15]. Raftari and his colleague (2012) have studied Homotopy analysis method (HAM) for MHD viscoelastic fluid flow and heat transfer in a channel with a stretching wall [16]. Yildirim and his colleague (2012) have addressed analytical solution of MHD stationary point flow in porous media by means of the Homotopy perturbation method [17]. Rashidi and his colleague (2010) have addressed analytic approximate solutions for unsteady boundary layer

flow and heat transfer in a stretching sheet by Homotopy perturbation method [18]. The analytical solutions of MHD free convective flow and mass transfer over a stretching sheet with chemical reaction have been done by Joneidi et al. (2010) [19]. Sajid and his colleague (2008) have performed the comparison of HAM and HPM methods in nonlinear heat conduction and convection equations [20]. In this research, it has been investigated the analytical solution of the steady MHD free convection flow over a semi-infinite flat vertical plate moving in a porous medium with viscous dissipation. The governing equations in this problem have been transformed into dimensionless equations with certain boundary conditions, using dimensionless quantities and these dimensionless equations have been solved by solving differential equations directly and using the perturbation method.

2. Mathematical Analysis

In this problem, a steady incompressible two-dimensional flow with a various viscosity is placed over a flat plate. It is assumed that the plate length is infinite and it is embedded in a porous medium. The semi-infinite flat plate is located vertically along the x-axis and the fluid flow is over the plate along the x-axis. The y-axis is a normal vector perpendicular to the plate. A magnetic field is introduced along the y-axis and perpendicular to the plate, and its strength is assumed to be negligible. The desired plate temperature is Tw, and the ambient temperature is around T∞. Heat transfer takes place due to the difference in temperature between the plate and the environment (Tw > T∞). Also, the desired plate concentration is Cw, and the environment concentration is C∞ (Cw > C∞). Fluid Magnetic Flow will be generated due to the magnetic field, so the magnetic Reynolds number should be taken into consideration, but since the electrical conductivity is very small, it is assumed that no voltage has been applied and accordingly, the magnetic Reynolds number is negligible and the fluid properties can be assumed to be constant.

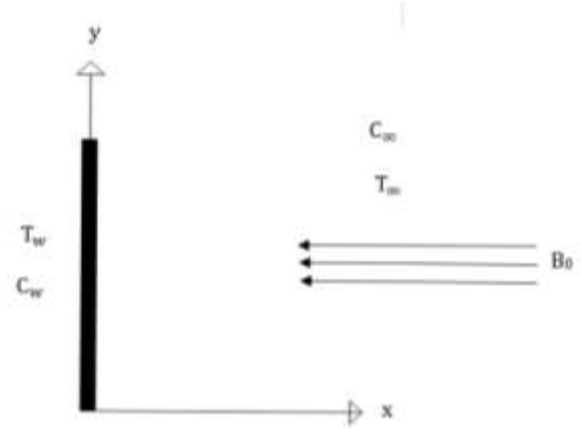

Fig. 1. Physical scheme of the plate and coordinate system

The governing equations include four equations that are continuity, momentum (Navier-Stokes), energy and concentration which are as follows:

Continuity equation:

$$\frac{\partial u}{\partial x}+\frac{\partial v}{\partial y}=0 \quad (1)$$

Momentum (Navier-Stokes) equation:

$$u\frac{\partial u}{\partial x}+v\frac{\partial u}{\partial y}=\nu\frac{\partial^2 u}{\partial y^2}+gB(T-T_\infty)+gB^*(C-C_\infty)-\frac{\sigma B_0^2}{\rho}u-\frac{\nu}{K'}u \quad (2)$$

Energy equation:

$$u\frac{\partial T}{\partial x}+v\frac{\partial T}{\partial y}=\alpha\frac{\partial^2 T}{\partial y^2}+\frac{D_m k_T}{C_s C_P}\frac{\partial^2 C}{\partial y^2}+\frac{\nu}{C_P}\left(\frac{\partial u}{\partial y}\right)^2 \quad (3)$$

Concentration equation:

$$u\frac{\partial C}{\partial x}+v\frac{\partial C}{\partial y}=D_m\frac{\partial^2 C}{\partial y^2}+\frac{D_m k_T}{T_m}\frac{\partial^2 T}{\partial y^2} \quad (4)$$

And boundary conditions are:

$$u=U_0, v=v_0(x), T=T_w, C=C_w \quad \rightarrow \quad y=0$$
$$u\rightarrow 0, v\rightarrow 0, T\rightarrow T_\infty, C\rightarrow C_\infty \quad \rightarrow \quad y\rightarrow\infty \quad (5)$$

Here, U_0 is uniform velocity of the plate, and $v_0(x)$ is suction velocity in the plate; u and v are velocity components in the direction of x and y, respectively; ρ is fluid density; g is acceleration of gravity, B and B^* are developed heat and concentration coefficients, respectively; K' is permeability of porous medium, T is the fluid temperature in the boundary layer; ν is kinematic viscosity; σ is fluid conductivity; T∞ is fluid temperature away from the plate; α is thermal penetration; C is concentration within the boundary layer; C_w is fluid concentration away from the plate; B0 is induction magnet; K is thermal conductivity; Cp is specific heat at constant pressure; KT is thermal emission ratio; Cs is concentration sensitivity; Tm is mean temperature and Dm is mass diffusion.

Using the dimensionless quantities, Multivariate Partial Differential Equations (MPDE) have been converted to Ordinary Differential Equations (ODE) with one variable. The dimensionless quantities are presented below for non-dimensionalization.

$$\eta=y\sqrt{\frac{U_0}{2\nu x}},\psi=\sqrt{\nu x U_0}f(\eta),\theta(\eta)=\frac{T-T_\infty}{T_w-T_\infty},\phi(\eta)=\frac{C-C_\infty}{C_w-C_\infty},u=\frac{\partial\psi}{\partial y},v=-\frac{\partial\psi}{\partial x}$$

$$G_r=\frac{gB(T_w-T_\infty)2x}{U_0^2},G_m=\frac{gB^*(C_w-C_\infty)2x}{U_0^2},M=\frac{2\sigma B_0^2 x}{\rho U_0},k=\frac{2\nu x}{K'U_0},S_c=\frac{\nu}{D_m}$$

$$P_r=\frac{\nu\rho C_P}{k},E_c=\frac{U_0^2}{C_P(T_w-T_\infty)},D_u=\frac{D_m k_T(C_w-C_\infty)}{C_s C_P(T_w-T_\infty)},S_r=\frac{D_m k_T(T_w-T_\infty)}{\nu T_m(C_w-C_\infty)}$$

(6)

Here, ψ is flow function, θ is dimensionless temperature function, ϕ is dimensionless concentration, G_r is thermal Grashof number, G_m is modified Grashof number, M is magnetic field parameter, k is permeability parameter, S_c is Schmidt number, P_r is Prandtl number, E_c is Eckert number, D_u is Dufour number, S_r is Soret number, f is the dimensionless flow function.

After non-dimensionalization, three equations including momentum (Navier-Stokes), energy, and concentration will be written in the form of the following dimensionless equations.

$$f''' + ff'' + G_r\theta + G_m\phi - (M + k)f' = 0 \quad (7)$$

$$\theta'' + P_r f\theta' + P_r D_u \phi'' + P_r E_c f''^2 = 0 \quad (8)$$

$$\phi'' + S_c f\phi' + S_c S_r \theta'' = 0 \quad (9)$$

The governing boundary conditions in the non-dimensional mode are:

$$\begin{aligned} &f = f_w, f' = 1, \theta = 1, \phi = 1 \quad \rightarrow \quad \eta = 0 \\ &f' \rightarrow 0, \theta \rightarrow 0, \phi \rightarrow 0 \quad \rightarrow \quad \eta \rightarrow \infty \end{aligned} \quad (10)$$

3. Solution of the problem:

Since the equations governing on the problem are differential equations higher than one, they are solved by direct method using perturbation technique. These equations are ordinary and non-homogeneous ones. So first, we write the governing equations (7)-(9) in homogeneous mode (zero mode) as follows:

$$f_0''' + ff_0'' - (M + k)f_0' = 0 \quad (11)$$

$$\theta_0'' + P_r f\theta_0' = 0 \quad (12)$$

$$\phi_0'' + S_c f\phi_0' = 0 \quad (13)$$

The boundary conditions for zero mode are equal to:

$$\begin{aligned} &f_0 = f_w, f_0' = 1, \theta_0 = 1, \phi_0 = 1 \quad \rightarrow \quad \eta = 0 \\ &f_0' \rightarrow 0, \theta_0 \rightarrow 0, \phi_0 \rightarrow 0 \quad \rightarrow \quad \eta \rightarrow \infty \end{aligned} \quad (14)$$

In the following, equations (7)-(9) are written in the first non-homogeneous mode (first mode).

$$f_1''' + ff_1'' - (M + k)f_1' = -G_r\theta_1 - G_m\phi_1 \quad (15)$$

$$\theta_1'' + P_r f\theta_1' = -P_r D_u \phi_1'' - P_r E_c f_0''^2 \quad (16)$$

$$\phi_1'' + S_c f\phi_1' = -S_c S_r \theta_0'' \quad (17)$$

According to the perturbation technique, the boundary conditions are homogenous for "first mode" in all cases and therefore,

Boundary conditions for "first mode" are as follows:

$$\begin{aligned} &f_1 = 0, f_1' = 0, \theta_1 = 0, \phi_1 = 0 \quad \rightarrow \quad \eta = 0 \\ &f_1' \rightarrow 0, \theta_1 \rightarrow 0, \phi_1 \rightarrow 0 \quad \rightarrow \quad \eta \rightarrow 0 \end{aligned} \quad (18)$$

And also, equations (19)-(21) in the second non-homogeneous mode (second mode) are written as follows:

$$f_2''' + ff_2'' - (M + k)f_2' = -G_r\theta_2 - G_m\phi_2 \quad (19)$$

$$\theta_2'' + P_r f\theta_2' = -P_r D_u \phi_2'' - P_r E_c f_1''^{\,2} \quad (20)$$

$$\phi_2'' + S_c f\phi_2' = -S_c S_r \theta_1'' \quad (21)$$

Boundary conditions for the second mode are as follows:

$$f_2 = 0, f_2' = 0, \theta_2 = 0, \phi_2 = 0 \quad \rightarrow \quad \eta = 0$$

$$f_2' \rightarrow 0, \theta_2 \rightarrow 0, \phi_2 \rightarrow 0 \quad \rightarrow \quad \eta \rightarrow 0 \quad (22)$$

Now, the general solutions, the first private solutions and the second private solutions for the three equations including momentum (Navier-Stokes), energy and concentration will be obtained from solving equations (11)-(13), (15)-(17), (19)-(21), respectively. The solutions obtained from solving the homogeneous equations (zero mode), the first non-homogeneous ones (first mode) and the second non-homogeneous ones (second mode) are as follows:

$$f_0' = e^{(k_1)\eta} \quad (23)$$

$$\theta_0 = e^{(k_2)\eta} \quad (24)$$

$$\phi_0 = e^{(k_3)\eta} \quad (25)$$

$$f_1' = L_{25}e^{(k_2)\eta} + L_{26}e^{(k_2)\eta} + L_{27}e^{(2k_1)\eta} + L_{28}e^{(k_2)\eta} \quad (26)$$

$$\theta_1 = L_5 e^{(2k_1)\eta} + L_6 e^{(k_2)\eta} \quad (27)$$

$$\phi_1 = L_1 e^{(k_2)\eta} \quad (28)$$

$$f_2' = L_{29}e^{(k_2)\eta} + 2L_{30}e^{(k_2)\eta} + L_{31}e^{(k_2)\eta} + L_{32}e^{(k_2)\eta} + L_{33}e^{(k_2)\eta}$$
$$+L_{34}e^{(k_1)\eta} + L_{35}e^{(k_1)\eta} + 2L_{36}e^{(2k_2)\eta} + L_{37}e^{(2k_2)\eta} + L_{38}e^{(2k_2)\eta}$$
$$+L_{39}e^{(2k_2)\eta} + L_{40}e^{(2k_2)\eta} + 2L_{41}e^{(2k_2)\eta} + L_{42}e^{(2k_2)\eta} + L_{43}e^{(2k_2)\eta}$$
$$+L_{44}e^{(2k_2)\eta} + L_{45}e^{(2k_2)\eta} + L_{46}e^{(4k_1)\eta} + L_{47}e^{(k_2+2k_1)\eta} + L_{48}e^{(k_2+2k_1)\eta}$$
$$+L_{49}e^{(k_2+2k_1)\eta} + L_{50}e^{(k_2+2k_1)\eta} + L_{51}e^{(2k_1+k_2)\eta} \quad (29)$$

$$\theta_2 = L_7 e^{(k_2)\eta} + L_8 e^{(k_2)\eta} + L_9 e^{(k_2)\eta} + L_{10}e^{(k_1)\eta} + 2L_{11}e^{(2k_2)\eta}$$
$$+L_{12}e^{(2k_2)\eta} + L_{13}e^{(4k_1)\eta} + L_{14}e^{(2k_2)\eta} + L_{15}e^{(2k_2)\eta} + L_{16}e^{(2k_2)\eta}$$
$$+L_{17}e^{(k_2+2k_1)\eta} + L_{18}e^{(2k_2)\eta} + L_{19}e^{(2k_2)\eta} + L_{20}e^{(k_2+2k_1)\eta} + L_{21}e^{(2k_2)\eta}$$
$$+L_{22}e^{(k_2+2k_1)\eta} + L_{23}e^{(2k_2)\eta} + L_{24}e^{(2k_1+k_2)\eta} \quad (30)$$

$$\phi_2 = L_2 e^{(k_2)\eta} + L_3 e^{(k_2)\eta} + L_4 e^{(2k_1)\eta} \quad (31)$$

Finally, the solutions obtained from solving equations in zero, first and second modes are written in the form of Taylor series, as follows:

$$f' = f_0' + E_c(f_1') + E_c^2(f_2') + \cdots + E_c^n(f_n') \quad (32)$$

$$\theta = \theta_0 + E_c(\theta_1) + E_c^2(\theta_2) + \cdots + E_c^n(\theta_n) \quad (33)$$

$$\phi = \phi_0 + E_c(\phi_1) + E_c^2(\phi_2) + \cdots + E_c^n(\phi_n) \quad (34)$$

And, since E_c<<1, it can be considered equal to ε (E_c = ε) [15].

4. Results and Discussion:

In the previous section of this study, it was dealt with solving the equations governing on the problem by applying existing boundary conditions through which it was obtained the relations related to the involved parameters. The numerical values of the parameters involved in the obtained equations have been considered in accordance with the following table:

Table 1. The numerical value of the skin-friction coefficient of the Nusselt number and Sherwood number according to D_u=0.2, S_r=1.0, E_c=0.01, P_r=0.71 and S_c=0.6 [11].

G_r	G_m	M	k	f_w	C_f	Nu	Sh
2.0	2.0	0.5	0.5	0.5	0.82302	0.86186	0.43622
4.0	2.0	0.5	0.5	0.5	1.68650	0.90193	0.46479
2.0	4.0	0.5	0.5	0.5	1.88533	0.91883	0.47943
2.0	2.0	1.0	0.5	0.5	0.49068	0.84005	0.42136
2.0	2.0	0.5	1.0	0.5	0.48781	0.83956	0.41984
2.0	2.0	0.5	0.5	1.0	0.51154	1.09368	0.47301

Table 2. The numerical value of the skin-friction coefficient of the Nusselt number and Sherwood number according to G_r=2.0, G_m=2.0, M=0.5, k=0.5 and f_w=0.5 [11].

P_r	E_c	D_u	S_c	S_r	C_f	Nu	Sh
0.71	0.01	0.2	0.6	1.0	0.82302	0.86186	0.43622
1.0	0.01	0.2	0.6	1.0	0.75371	1.10872	0.29084
0.71	0.02	0.2	0.6	1.0	0.82406	0.85906	0.43788
0.71	0.01	0.4	0.6	1.0	0.84053	0.82924	0.45734
0.71	0.01	0.2	0.78	1.0	0.77315	0.84694	0.49949
0.71	0.01	0.2	0.6	2.0	1.00844	0.93308	0.29313

In the above tables, changing each of the parameters S_c, S_r, D_u, E_c, P_r, k, M, G_r and G_m causes a change in Sherwood Number (Sh), Nusselt Number (Nu) and skin-fraction coefficient (C_f) and the numerical value of these changes has been explicitly stated. The relations of calculation of the three non-dimensional numbers are as follows:

$$C_f = \left(\frac{\partial^2 f}{\partial \eta^2}\right)_{\eta=0} = f''(0) \quad (35)$$

$$Nu = -\left(\frac{\partial \theta}{\partial \eta}\right)_{\eta=0} = -\theta'(0) \quad (36)$$

$$\mathrm{Sh} = -\left(\frac{\partial \phi}{\partial \eta}\right)_{\eta=0} = -\phi'(0) \tag{37}$$

Formulas 35, 36 and 37 have been taken from reference [1].

We know that Grashof number (G_r) represents the ratio of the buoyancy force to viscosity force in the boundary layer. This number is used to distinguish between laminar and turbulent flow in the free convection heat transfer, G_r =2, 4; so that the effect of Grashof number on the velocity distribution in terms of η is shown in Fig.2.

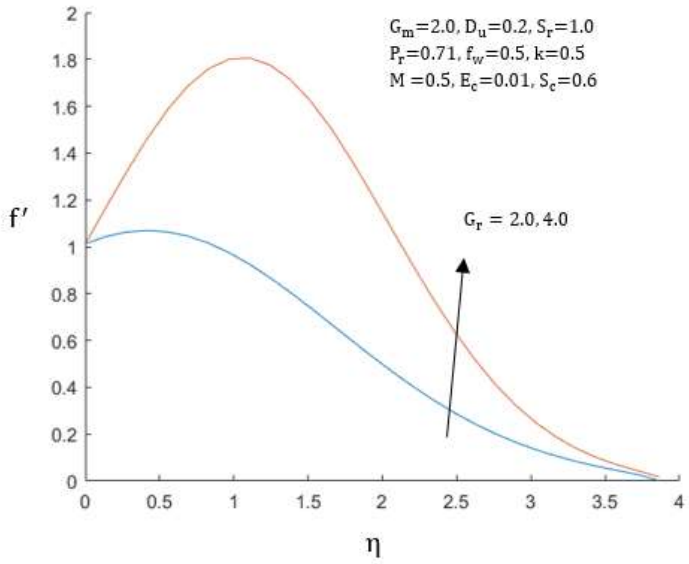

Fig. 2. velocity profile for G_r

The modified Grashof number (G_m) represents the relative value of concentration buoyancy force to viscous hydrodynamic force in the boundary layer [7]. This Grashof number is the same as the dimensionless thermal Grashof number (G_r). As this number increases, velocity profile rises and the increased η leads to the reduced velocity profile. In other words, increased viscosity reduces the thickness of the boundary layer. The behavior of both velocity profiles is the same for Grashof and modified Grashof numbers, except that velocity for the modified Grashof profile is less than thermal Grashof number (G_r) at the peak of velocity

profile. In Fig.3, the velocity distribution is indicated in terms of η for two modified Grashof numbers.

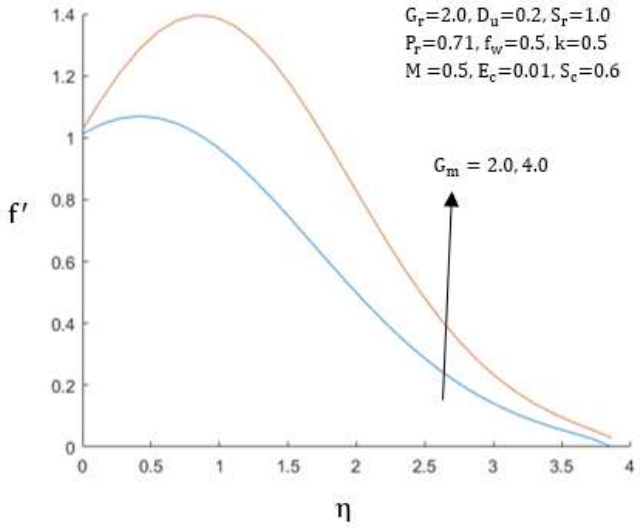

Fig. 3. velocity profile for G_m

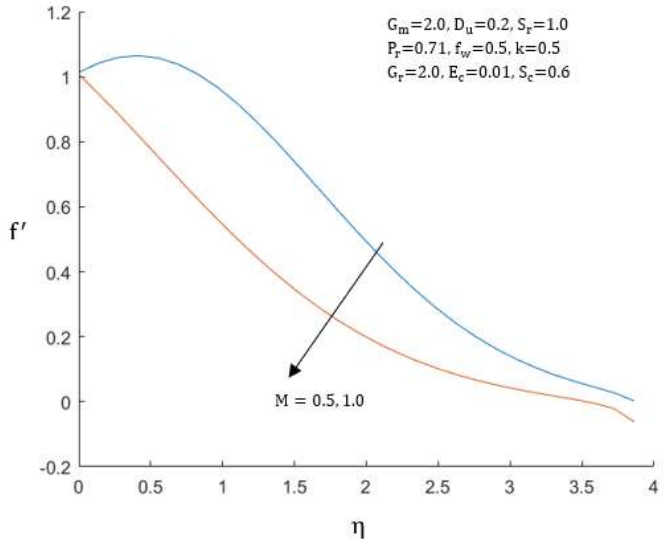

Fig. 4. velocity profile for *M*

The magnetic parameter (M) applies a delayed force on free convection flow and the velocity and the thickness of the boundary layer are reduced by increasing magnetic parameter [3]. In Fig. 4, the velocity distribution is indicated in terms of η for two magnetic parameters.

The magnetic permeability parameter (k) is i

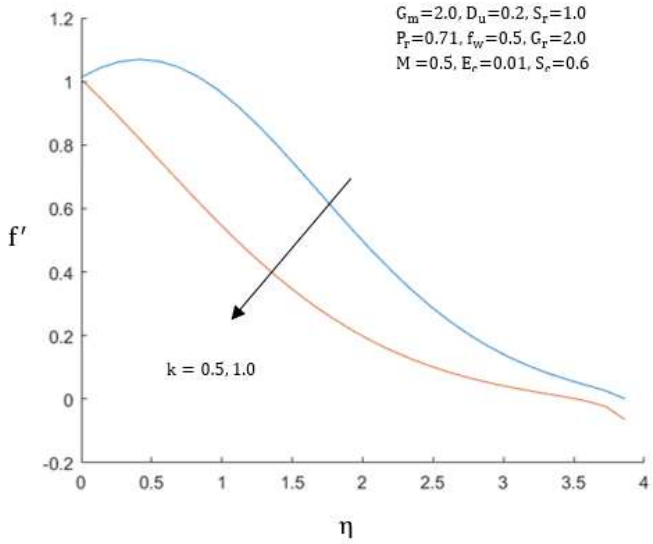

Fig. 5. velocity profile for *k*

nversely proportional to the actual permeability in a porous medium [7]. The increased magnetic permeability parameter reduces the velocity and as a result, it causes a decline in the velocity profile, which is due to the increased resistance of the porous medium. In Fig. 5, the velocity distribution is shown in terms of η for the magnetic permeability parameter.

The dimensionless Prandtl number (P_r) represents the ratio of velocity penetration factor to thermal penetration factor. The relative thickness of boundary layers of velocity and heat is described by the Prandtl number. If P_r <<1, heat will be dispersed very quickly and the heat boundary layer will be thicker than the velocity boundary layer. If P_r >>1, the momentum will be dissipated much faster than heat and the thermal boundary layer will be thinner than the velocity boundary layer. In Fig.6, the velocity distribution is shown in terms of η for two Prandtl numbers.

The increased Prandtl number reduces the velocity and as a result, the velocity and the temperature profiles will be declined by increasing Prandtl number. Figure 7 indicates a decline in the temperature profile due to the increased Prandtl number.

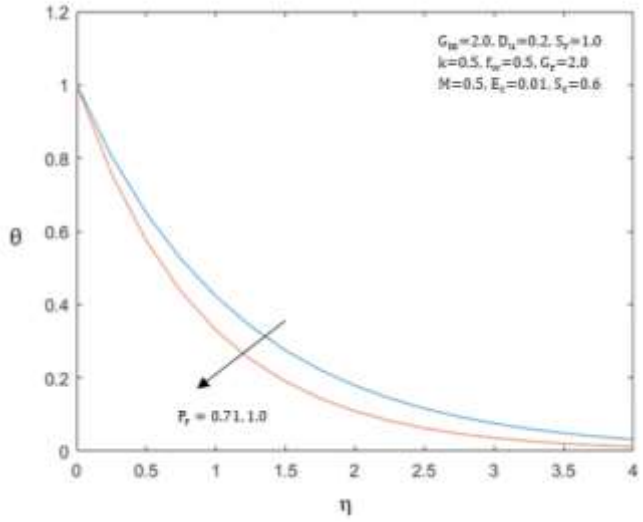

Fig. 6. Velocity profile for P_r

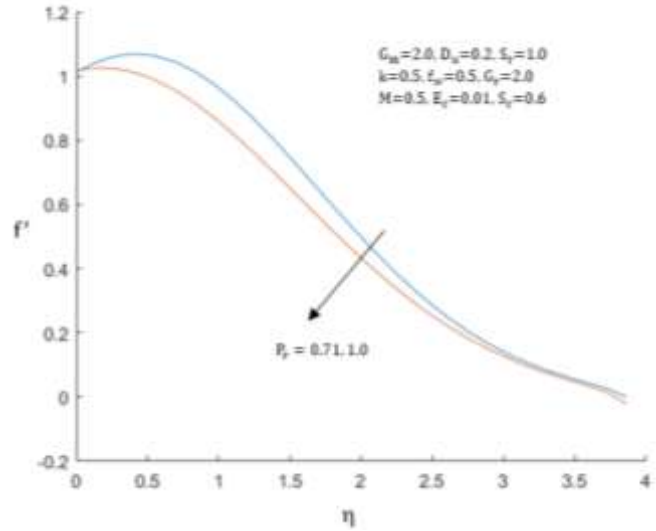

Fig. 7. Velocity profile for P_r

Therefore, the heat dissipation from the hot plate in small Prandtl numbers is greater than large ones. As a result, compared to larger Prandtl numbers, small Prandtl numbers have the thicker boundary layers, and therefore, they have the heat transfer lower than the larger Prandtl numbers.

Eckert number is a dimensionless number used in the high-speed heat transfer problems. Eckert number is a criterion of the ratio of kinetic energy of the fluid to the enthalpy difference in the thermal boundary layer. When the Eckert number is greater than zero (positive), it works as a coolant; and when the dissipated heat is higher, it causes an increase in fluid velocity. The small Eckert numbers are usually ignored.

According to the diagram in Fig.8, the velocity profile has an ascending mode and the velocity increases by increasing the Eckert number; according to the diagram in Fig.9, the temperature profile has an ascending mode and the temperature increases by increasing the Eckert number.

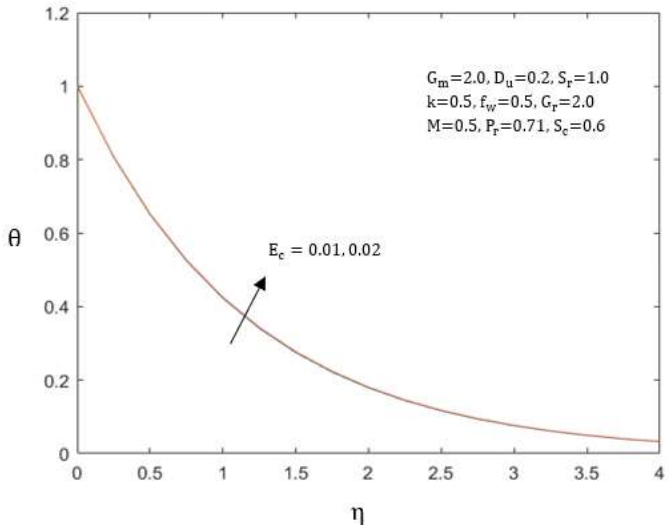

Fig. 8. The velocity profile for E_c

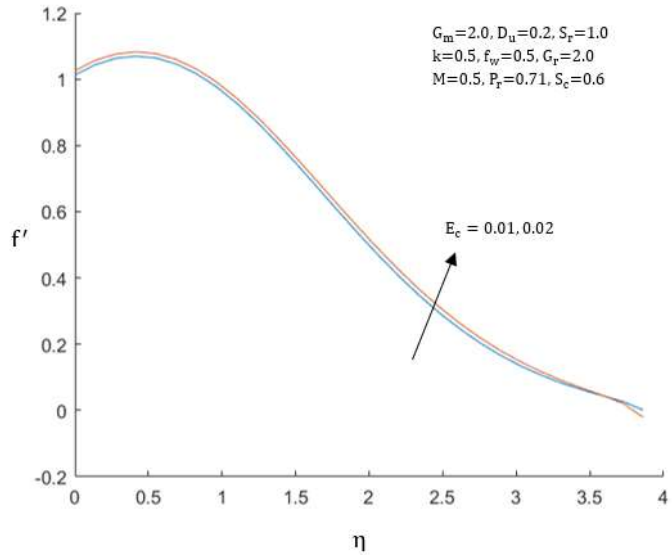

Fig. 9. Temperature profile for E_c

Dufour number is a dimensionless quantity that is equal to the ratio of the concentration gradient to the flux of thermal energy in the flow. Increased Dufour number causes an increase in the velocity and temperature in the boundary layer [11]. In the Dufour number, the concentration gradient causes temperature change, and it can be said that the density affects the Dufour number. When the Dufour number increase, the velocity at the beginning of the boundary layer increases due to the low viscosity effects, and when the viscosity effect increases at the end of the boundary layer, the velocity becomes closer to zero. In fact, it can be said that increased viscosity reduces the velocity at the edges of the boundary layer. The diagram in fig.10 indicates the velocity distribution in terms of η for the Dufour number. Also, Fig. 11 shows the temperature profile which increases by increased Dufour number.

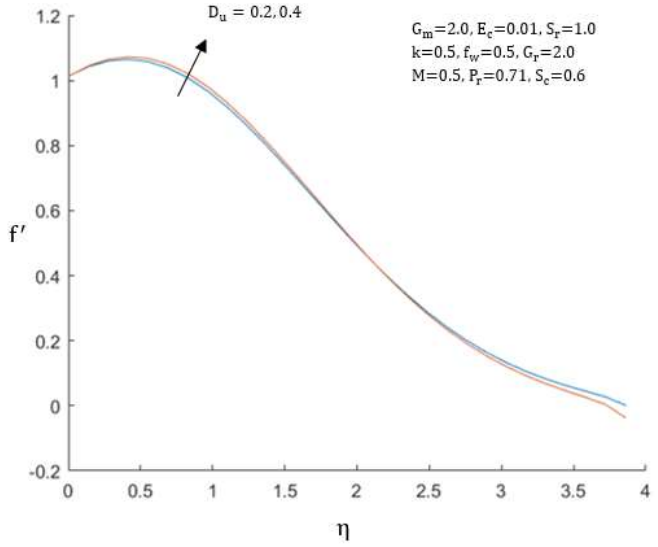

Fig. 10. The velocity profile for D_u

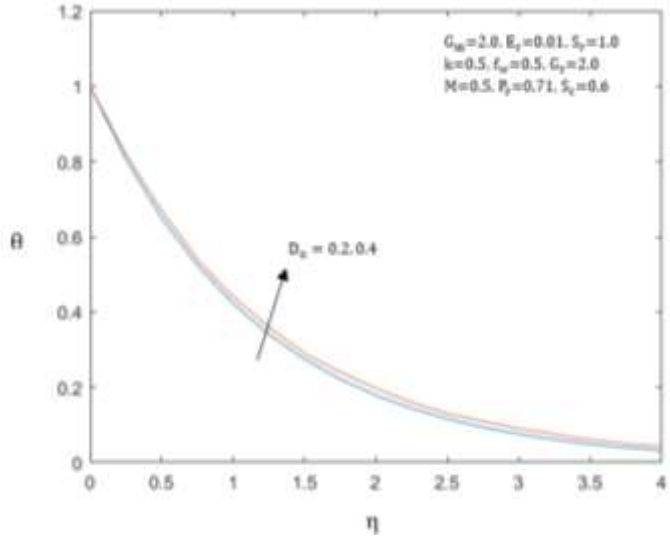

Fig. 11. The temperature profile for D_u

Soret is a dimensionless number expressed in the density domain. Soret number represents the effects of the temperature gradient induced to the effects of mass penetration. In fact, if the density difference is considerable, it can create the Soret effect. When the Soret number increases, the density-dependent concentration will be increased and also, the velocity will increase with increasing the Soret number. According to the diagram in Fig.12, the velocity distribution has been shown in terms of η for two Soret numbers, as well as the diagram of Fig.13 indicates the concentration profile in terms of η for two Soret numbers.

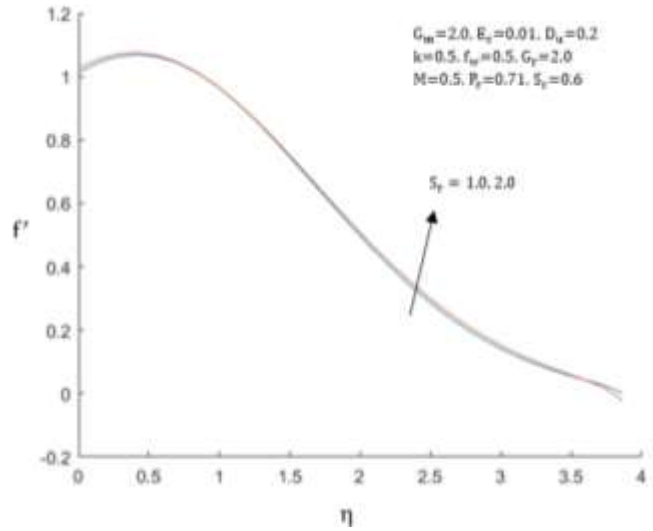

Fig. 12. The velocity profile for S_r

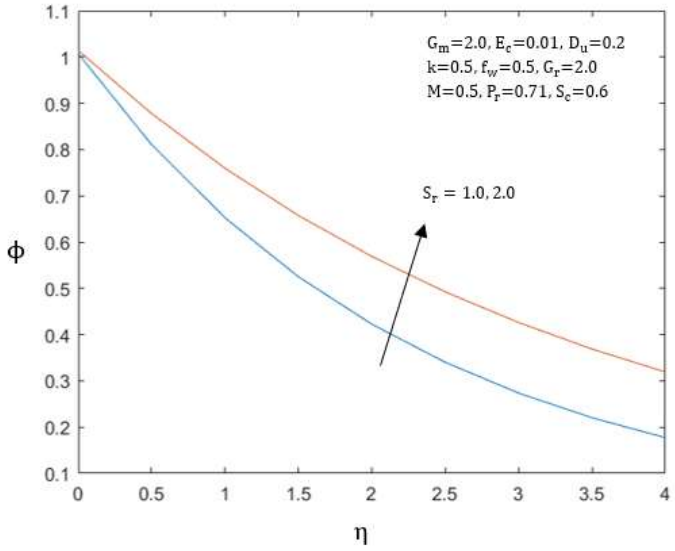

Fig. 13. The concentration profile for S_r

The Schmidt number (S_c) is a dimensionless number representing the ratio of the momentum penetration (motion) to the mass penetration (concentration). This number, as an effective quantity, is the ratio of the velocity of fluid flow to the mass transfer of the

concentration boundary layer [7]. Due to the floating property, the concentration and velocity of the fluid are reduced, which increased Schmidt number can also reduce both of them. According to the Fig.14, the velocity distribution has been shown in terms of η for two Schmidt numbers and also, the concentration profile in terms of η for two Schmidt numbers is shown in Fig.15.

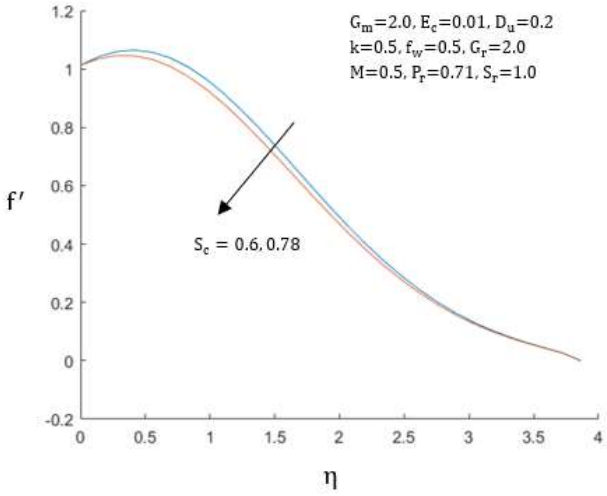

Fig. 14. The velocity profile for S_c

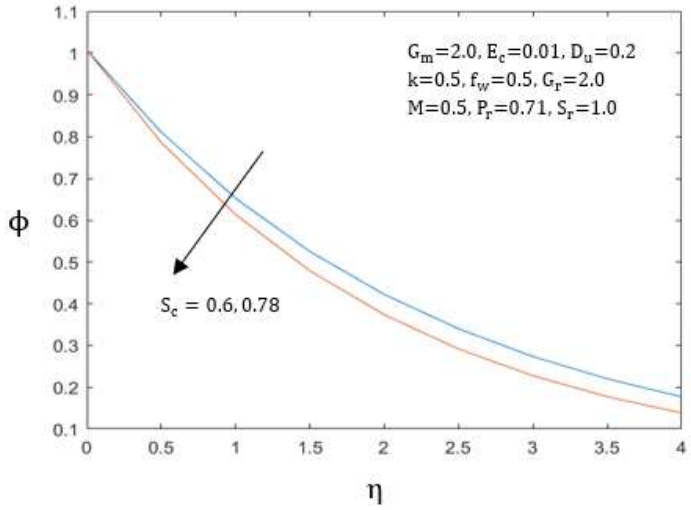

Fig. 15. The concentration profile for S_c

(fw) is the dimensionless suction velocity parameter. As fw increases, thickness of the heat boundary layer, the temperature, velocity and concentration profiles are reduced [21]. The diagrams of figures (16), (17) and (18) show distribution of velocity, temperature, and concentration in terms of η for two suction parameters fw, respectively.

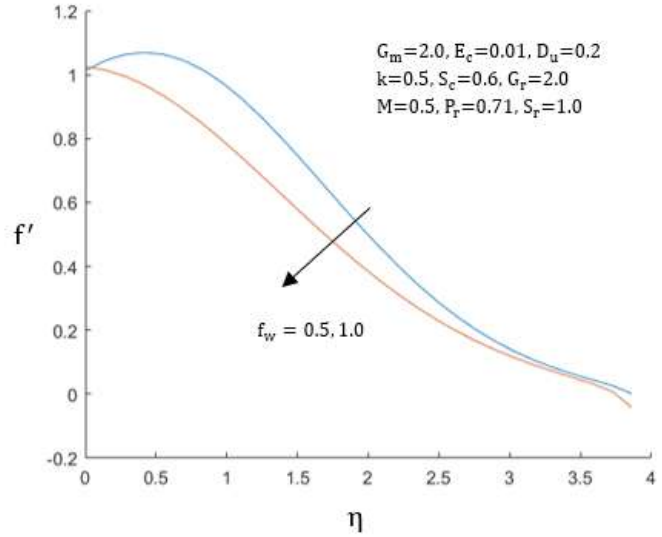

Fig. 16. The velocity profile for f_w

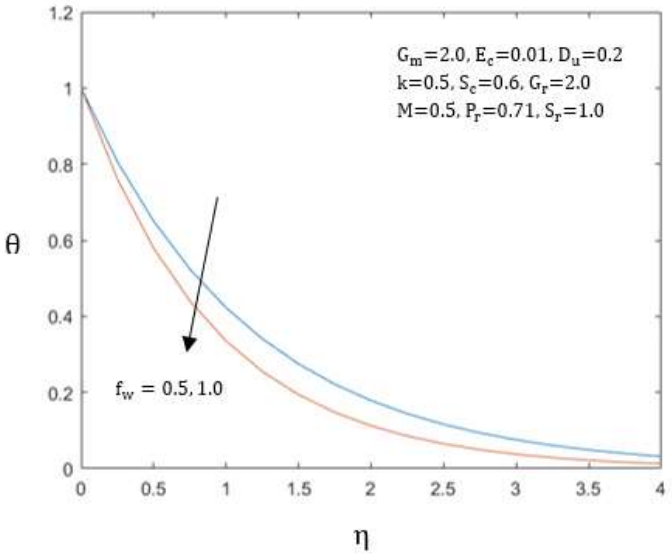

Fig. 17. The temperature profile for f_w

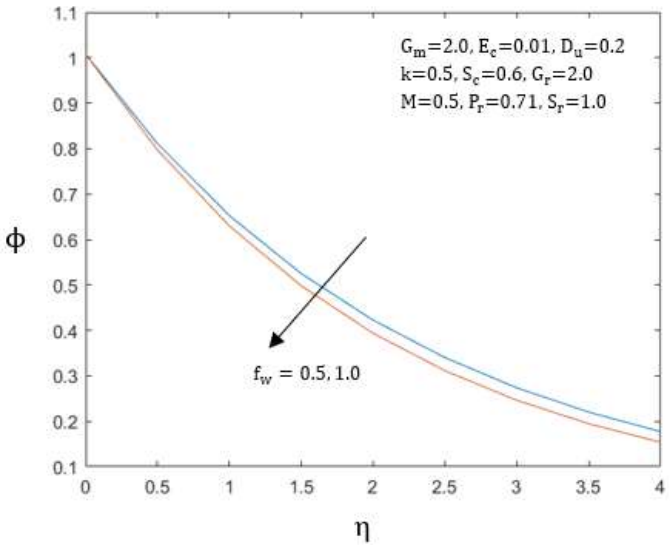

Fig. 18. Concentration profile for f_w

5. Conclusion

In this paper, it has been discussed the analytical solution of steady MHD free convection flow past a semi-infinite flat vertical plate moving in a porous medium with viscous dissipation. Finally, we have examined the results of this analysis in the form of three "concentration, temperature and velocity" profiles and the effects of different parameters such as Schmidt, Grashof and etc. numbers in the three profiles:
The results for concentration profile:

I. As Schmidt number (S_c) increases, the concentration profile is reduced.
II. As Soret number (S_r) increases, the concentration profile is reduced.
III. As section parameter (fw) increases, the concentration profile is reduced.

The results for the temperature profile:

I. As Prandtl number (P_r) increases, the temperature profile is reduced.
II. As Eckert number (E_c) increases, the temperature profile is increased.
III. As Dufour number (D_u) increases, the temperature profile is increased.
IV. As suction parameter (fw) increases, the temperature profile is reduced.

The results for the velocity profile:

I. As Dufour number (D_u) increases, the velocity profile is increased.
II. As Soret number (S_r) increases, the velocity profile is increased.
III. As Eckert number (E_c) increases, the velocity profile is increased.
IV. As Prandtl number (P_r) increases, the velocity profile is reduced.
V. As Schmidt number (S_c) increases, the velocity profile is reduced.
VI. As the magnetic permeability (k) increases, the velocity profile is reduced.
VII. As Grashof number (G_m) increases, the velocity profile is increased.
VIII. As Grashof number (G_r) increases, the velocity profile is increased.

IX. As the magnetic parameter number (M) increases, the velocity profile is reduced.
X. As the suction parameter (fw) increases, the velocity profile is reduced.

Appendix:

$$L_1 = S_r P_r$$

$$L_2 = -\frac{2P_r^2 S_r^2 D_u}{f}$$

$$L_3 = P_r^3 D_u S_r^2 \eta$$

$$L_4 = \frac{E_c S_r\left(-f - \sqrt{M+k}\right)}{f^2}$$

$$L_5 = -\frac{E_c\left(-f - \sqrt{M+k}\right)}{2f}$$

$$L_6 = P_r^2 D_u S_r\, \eta$$

$$L_7 = 2P_r^4 S_r^2 D_u\, \eta$$

$$L_8 = 2P_r^4 S_r^2 D_u^2\, \eta$$

$$L_9 = -P_r^5 S_r^2 D_u^2 f\, \eta^2$$

$$L_{10} = -\frac{2E_c S_r D_u\left(-f - \sqrt{M+K}\right)^2}{f^2}$$

$$L_{11} = \frac{P_r^3 S_r^2 D_u^2 E_c}{2f^2(M+k)^2}$$

$$L_{12} = \frac{P_r^5 S_r^2 D_u^2 E_c}{(M+k)^2}\eta^2$$

$$L_{13} = -\frac{G_r^2 E_c^3\left(-f - \sqrt{M+K}\right)^3}{4f^3(M+k)^2}$$

$$L_{14} = \frac{G_m^2 S_r^2 P_r^3 E_c}{2(M+k)^2}$$

$$L_{15} = \frac{P_r^3 S_r^2 D_u^2 E_c}{f^2(M+k)^2}$$

$$L_{16} = -\frac{P_r^4 S_r^2 D_u^2 E_c}{f(M+k)^2}$$

$$L_{17} = \frac{2P_r^2 E_c^2 S_r D_u G_r\left(-f - \sqrt{M+K}\right)^2}{f^2(M+k)^2\left(-P_r f + 2\left(-f - \sqrt{M+k}\right)\right)}$$

$$L_{18} = \frac{P_r^3 D_u S_r^2 E_c}{f(M+k)^2}$$

$$L_{19} = -\frac{P_r^4 D_u^2 S_r^2 E_c}{f(M+k)^2}$$

$$L_{20} = \frac{2P_r^2 E_c^2 S_r D_u\left(-f - \sqrt{M+K}\right)^2}{f^2(M+k)^2\left(-P_r f + 2\left(-f - \sqrt{M+k}\right)\right)}$$

$$L_{21} = \frac{P_r^3 S_r^2 E_c D_u G_m}{f(M+k)^2}$$

$$L_{22} = -\frac{2P_r^3 E_c^2 S_r D_u G_r\left(-f - \sqrt{M+K}\right)^2}{f(M+k)^2\left(-P_r f + 2\left(-f - \sqrt{M+k}\right)\right)}\eta$$

$$L_{23} = -\frac{P_r^4 S_r^2 E_c D_u G_m}{(M+k)^2}\eta$$

$$L_{24} = \frac{2P_r^2 E_c^2 S_r G_r G_m\left(-f - \sqrt{M+K}\right)^2}{f(M+k)^2\left(-P_r f + 2\left(-f - \sqrt{M+k}\right)\right)}$$

$$L_{25} = \frac{D_u P_r S_r G_r}{f(M+k)}$$

$$L_{26} = -\frac{P_r^2 D_u S_r G_r}{(M+k)}\eta$$

$$L_{27} = \frac{E_c G_r\left(-f - \sqrt{M+k}\right)}{2f(M+k)}$$

$$L_{28} = \frac{P_r S_r G_m}{(M+k)}$$

$$L_{29} = -\frac{P_r^3 S_r^2 D_u G_r}{f(M+k)}$$

$$L_{30} = \frac{2P_r^4 S_r^2 D_u G_r}{(M+k)}\eta$$

$$L_{31} = -\frac{2P_r^3 S_r^2 D_u G_r}{f(M+k)}$$

$$L_{32} = \frac{2P_r^4 D_u^2 S_r^2 G_r}{(M+k)}\eta$$

$$L_{33} = -\frac{P_r^5 D_u^2 S_r^2 G_r f}{(M+k)}\eta^2$$

$$L_{34} = \frac{E_c G_r S_r D_u\left(-f - \sqrt{M+k}\right)}{f^2}$$

$$L_{35} = \frac{E_c G_r S_r D_u \left(-f - \sqrt{M + K}\right)^2}{f^2} \eta$$

$$L_{36} = \frac{P_r^3 D_u^2 S_r^2 E_c G_r}{2f^2 (M + k)^3}$$

$$L_{37} = -\frac{P_r^4 D_u^2 S_r^2 E_c G_r}{f(M + k)^3} \eta$$

$$L_{38} = \frac{P_r^5 D_u^2 S_r^2 E_c G_r}{(M + k)^3} \eta^2$$

$$L_{39} = \frac{P_r^3 G_m^2 S_r^2 E_c G_r}{2(M + k)^3}$$

$$L_{40} = \frac{P_r^3 D_u^2 S_r^2 E_c G_r}{f^2 (M + k)^3}$$

$$L_{41} = -\frac{P_r^4 D_u^2 S_r^2 E_c G_r}{f(M + k)^3}$$

$$L_{42} = \frac{P_r^3 S_r^2 D_u E_c G_r}{f(M + k)^3}$$

$$L_{43} = \frac{P_r^3 S_r^2 D_u E_c G_r G_m}{f(M + k)^3}$$

$$L_{44} = \frac{P_r^3 S_r^2 D_u E_c G_r G_m}{2f(M + k)^3}$$

$$L_{45} = -\frac{P_r^4 S_r^2 D_u E_c G_r G_m}{(M + k)^3} \eta$$

$$L_{46} = -\frac{G_r^3 E_c^3 \left(-f - \sqrt{M + K}\right)^3}{4f^3 (M + k)^3}$$

$$L_{47} = -\frac{2P_r^2 G_r^2 E_c^2 D_u S_r \left(-f - \sqrt{M + K}\right)^2}{f^2 (M + k)^3 (-P_r f + 2\left(-f - \sqrt{M + k}\right))}$$

$$L_{48} = -\frac{2P_r^2 E_c^2 D_u S_r G_r \left(-f - \sqrt{M + K}\right)^2}{f^2 (M + k)^3 \left(-P_r f + 2\left(-f - \sqrt{M + k}\right)\right)}$$

$$L_{49} = \frac{2P_r^3 E_c^2 G_r^2 D_u S_r \left(-f - \sqrt{M + K}\right)^2}{f(M + k)^3 \left(-P_r f + 2\left(-f - \sqrt{M + k}\right)\right)^2}$$

$$L_{50} = \frac{2P_r^3 E_c^2 G_r^2 D_u S_r \left(-f - \sqrt{M + K}\right)^2}{f(M + k)^3 \left(-P_r f + 2\left(-f - \sqrt{M + k}\right)\right)} \eta$$

$$L_{51} = -\frac{2P_r^2 E_c^2 G_r^2 G_m S_r\left(-f-\sqrt{M+K}\right)^2}{(M+k)^3\left(2\left(-f-\sqrt{M+k}\right)-P_r f\right)}$$

$$K_1 = \left(-f-\sqrt{M+k}\right)$$

$$K_2 = (-P_r f)$$

$$K_3 = (-Scf)$$

REFERENCES

[1] Wahiduzzaman, M., Biswas, R., Ali, M. E., Khan, M. S., & Karim, I. (2015). Numerical Solution of MHD Convection and Mass Transfer Flow of Viscous Incompressible Fluid about an Inclined Plate with Hall Current and Constant Heat Flux. Journal of Applied Mathematics and Physics, 3(12), 1688.
[2] Wahiduzzaman, M., Khan, M. S., Karim, I., Biswas, P., & Uddin, M. S. (2015). MHD Flow of Fluid over a Rotating Inclined Permeable Plate with Variable Reactive Index. Physical Science International Journal, 6, 144-162.
[3] Khan, M. S., Karim, I., & Biswas, M. H. A. (2012). Non-Newtonian MHD mixed convective power-Law fluid flow over a vertical stretching sheet with thermal radiation, heat generation and chemical reaction effects. Academic Research International, 3(3), 80.
[4] Saha, L. K., Siddiqa, S., & Hossain, M. A. (2011). Effect of Hall current on MHD natural convection flow from vertical permeable flat plate with uniform surface heat flux. Applied Mathematics and Mechanics, 32(9), 1127-1146.
[5] Samad, M. A., & Mohebujjaman, M. (2009). MHD heat and mass transfer free convection flow along a vertical stretching sheet in presence of magnetic field with heat generation. Res. J. Appl. Sci. Eng. Technol, 1(3), 98-106.
[6] Das, S. S., Satapathy, A., Das, J. K., & Panda, J. P. (2009). Mass transfer effects on MHD flow and heat transfer past a vertical porous plate through a porous medium under oscillatory suction and heat source. International journal of heat and mass transfer, 52(25), 5962-5969.
[7] Aboeldahab, E. M., & Elbarbary, E. M. (2001). Hall current effect on magnetohydrodynamic free-convection flow past a semi-infinite vertical plate with mass transfer. International Journal of Engineering Science, 39(14), 1641-1652.
[8] Gangadhar, K. (2013). Soret and Dufour effects on hydro magnetic heat and mass transfer over a vertical plate with a convective surface boundary condition and chemical reaction. Journal of Applied Fluid Mechanics, 6(1), 95-105.
[9] Karim, M. E., Samad, M. A., & Hasan, M. M. (2012). Dufour and Soret effect on steady MHD flow in presence of Heat generation and magnetic field past an inclined stretching sheet. Open Journal of Fluid Dynamics, 2(3), 91.
[10] Tai, B. C., & Char, M. I. (2010). Soret and Dufour effects on free convection flow of non-Newtonian fluids along a vertical plate embedded in a porous medium with thermal radiation. International Communications in Heat and Mass Transfer, 37(5), 480-483.
[11] Reddy, M. G., & Reddy, N. B. (2010). Soret and Dufour effects on steady MHD free convection flow past a semi-infinite moving vertical plate in a porous medium with viscous dissipation. International Journal of Applied Mathematics and Mechanics, 6(1), 1-12.
[12] Tsai, R., & Huang, J. S. (2009). Numerical study of Soret and Dufour effects on heat and mass transfer from natural convection flow over a vertical porous medium with variable wall heat fluxes. Computational Materials Science, 47(1), 23-30.
[13] Postelnicu, A. (2004). Influence of a magnetic field on heat and mass transfer by natural convection from vertical surfaces in porous media considering Soret and Dufour effects. International Journal of Heat and Mass Transfer, 47(6), 1467-1472.
[14] Omowaye, A. J., Fagbade, A. I., & Ajayi, A. O. (2015). Dufour and soret effects on steady MHD convective flow of a fluid in a porous medium with temperature dependent

viscosity: Homotopy analysis approach. Journal of the Nigerian Mathematical Society, 34(3), 343-360.

[15] Raju, M. C., Reddy, N. A., & Varma, S. V. K. (2014). Analytical study of MHD free convective, dissipative boundary layer flow past a porous vertical surface in the presence of thermal radiation, chemical reaction and constant suction. Ain Shams Engineering Journal, 5(4), 1361-1369.

[16] Raftari, B., & Vajravelu, K. (2012). Homotopy analysis method for MHD viscoelastic fluid flow and heat transfer in a channel with a stretching wall. Communications in Nonlinear Science and Numerical Simulation, 17(11), 4149-4162.

[17] Yildirim, A., & Sezer, S. A. (2012). Analytical solution of MHD stagnation-point flow in porous media by means of the homotopy perturbation method. Journal of Porous Media, 15(1).

[18] Rashidi, M. M., & Pour, S. M. (2010). Analytic approximate solutions for unsteady boundary-layer flow and heat transfer due to a stretching sheet by homotopy analysis method. Nonlinear Analysis: Modelling and Control, 15(1), 83-95.

[19] Joneidi, A. A., Domairry, G., & Babaelahi, M. (2010). Analytical treatment of MHD free convective flow and mass transfer over a stretching sheet with chemical reaction. Journal of the Taiwan Institute of Chemical Engineers, 41(1), 35-43.

[20] Sajid, M., & Hayat, T. (2008). Comparison of HAM and HPM methods in nonlinear heat conduction and convection equations. Nonlinear Analysis: Real World Applications, 9(5), 2296-2301

[21] NAZARI, M. (2016). Thermal Non-Equilibrium Similarity Solution for Nanofluid Boundary Layer in a Porous Medium. Amirkabir Journal of Mechanical Engineering, 48(3), pp. 281–290.